Extending Bayesian RFS SLAM to Multi-Vehicle SLAM

Diluka Moratuwage*, Ba-Ngu Vo†, Danwei Wang* and Han Wang*
*School of Electrical and Electronic Engineering
Nanyang Technological University
Singapore
†Department of Electrical and Computer Engineering
Curtin University
Australia

***Abstract*—In this paper we present a novel solution to the Multi-Vehicle SLAM (MVSLAM) problem by extending the random finite set (RFS) based SLAM filter framework using two recently developed multi-sensor information fusion approaches. Our solution is based on the modelling of the measurements and the landmark map as RFSs and factorizing the MVSLAM posterior into a product of the joint vehicle trajectories posterior and the landmark map posterior conditioned the vehicle trajectories. The joint vehicle trajectories posterior is propagated using a particle filter while the landmark map posterior conditioned on the vehicle trajectories is propagated using a Gaussian Mixture (GM) implementation of the probability hypothesis density (PHD) filter.**

***Index Terms*—Multi-Robot, SLAM, PHD.**

I. Introduction

A number of Multi-Vehicle SLAM (MVSLAM) solutions are found in the robotics literature [1] [2] [3] [4] [5] [6] [7] developed by extending the conventional vector based mono-SLAM algorithms such as extended Kalman filter based SLAM (EKF-SLAM) [8], FastSLAM [9] and sparse extended information filter based SLAM (SEIF-SLAM) [10]. All these mono-SLAM algorithms solve the SLAM problem by propagating a posterior probability density of a vector consisting of the landmark map augmented with the vehicle state in time. Hence all such algorithms require solving certain additional sub-problems such as data association, clutter filtering and map management in order to produce a consistent solution. In addition, landmark detection uncertainty or data association uncertainty are not taken into account.

In order to address these issues in the conventional mono-SLAM solutions, random finite set (RFS) modelling was adopted. The very first RFS based SLAM solution was presented by Mullane et al. in [11], where they modelled the measurements and augmented vehicle-landmark map state as RFSs. The augmented vehicle-landmark map state was propagated in time using a probability hypothesis density (PHD) filter [12] [13] from which the state of the vehicle and the landmark locations were jointly estimated. Further improving their original solution, in [14] [15] Mullane et al. proposed a Rao-Blackwellised PHD filtering solution by factorizing the full SLAM posterior into a product of the vehicle trajectory posterior and the landmark map posterior conditioned on the vehicle treajectory. This solution addressed the map management, landmark detection uncertainty and false measurements (clutter) in a single filtering step by representing the landmark map and measurements as RFSs and modelling the landmark map transition model more natural and appropriate manner. Moreover this approach catered for propagation of vehicle trajectory posterior using a particle filter and the landmark map posterior conditioned on the vehicle trajectory using a Gaussian mixture (GM) implementation [16] of a PHD filter.

In this paper we present a new solution to the Multi-Vehicle SLAM (MVSLAM) problem by extending the RFS based SLAM filter framework. The proposed solution is based on the factorization of the full MVSLAM posterior into a product of the joint vehicle trajectories posterior and the landmark map posterior conditioned on the joint vehicle trajectories. The landmark map and the measurements are modelled as RFSs and the joint vehicle trajectories are propagated in time via a particle filter while the landmark conditioned on the vehicle trajectories is propagated using a GM implementation of a PHD filter. The key idea of this paper was originally presented at the IEEE ICRA workshop on "Stochastic Geometry in SLAM" in 2012. In this paper, we present a more complex simulation scenario and a comprehensive performance analysis is carried out by comparing the results with the MVSLAM solution proposed by Howard [4].

II. Random Finite Set Multi-Vehicle SLAM Problem

We illustrate the RFS Multi-Vehicle SLAM algorithm for the case of two vehicles although it can be extended into a larger number of robots using the methos we present here.

Let the landmark map be denoted by the set $M_k = \{m_{k,1}, m_{k,2}, ..., m_{k,l_k}\}$ at time k, where l_k denotes the number of landmarks present in the map. Let the time sequence of poses history of each vehicle be denoted by $X_{1:k}^{(r)} = [X_1^{(r)}, X_2^{(r)}, ..., X_k^{(r)}]^T$, where $X_k^{(r)}$ denotes the pose of vehicle r, at time k. Let the time sequence of sets of range measurements obtained using range and bearing sensors mounted on each vehicle be denoted by $Z_{1:k}^{(r)} = [Z_1^{(r)}, Z_2^{(r)}, ..., Z_k^{(r)}]$, where $Z_k^{(r)} = \{z_{k,1}^{(r)}, z_{k,2}^{(r)}, ..., z_{k,n_k^{(r)}}^{(r)}\}$ denotes the measurement

set received from vehicle r at time k, while $n_k^{(r)}$ denotes the number of measurements. Let $U_{1:k}^{(r)} = [U_1^{(r)}, U_2^{(r)}, ..., U_k^{(r)}]^T$ denote the time sequence of control commands applied to each vehicle $r, (r = 1, 2)$ upto time k, where $U_k^{(r)}$ denotes the control command applied at time k. The MVSLAM posterior probability distribution is then given by,

$$p_{k|k}(M_k, X_{1:k}^{(1)}, X_{1:k}^{(2)} | Z_{1:k}^{(1)}, Z_{1:k}^{(2)}, U_{1:k}^{(1)}, U_{1:k}^{(2)}, X_0^{(1)}, X_0^{(2)}) \quad (1)$$

where $X_0^{(1)}$ and $X_0^{(2)}$ respectively denote the initial poses of first and second vehicles.

III. Formulation of Proposed Random Finite Set Multi-Vehicle SLAM Solution

The Multi-Vehicle SLAM posterior (1) is evaluated by factorizing as a product of the joint vehicle poses posterior and the landmark map posterior conditioned on the vehicle poses as follows,

$$\begin{aligned} &p_{k|k}(M_k, X_{1:k}^{(1)}, X_{1:k}^{(2)} | Z_{1:k}^{(1)}, Z_{1:k}^{(2)}, U_{1:k}^{(1)}, U_{1:k}^{(2)}, X_0^{(1)}, X_0^{(2)}) \\ &= p_{k|k}(M_k | Z_{1:k}^{(1)}, Z_{1:k}^{(2)}, X_{0:k}^{(1)}, X_{0:k}^{(2)}) \\ &\times p_{k|k}(X_{1:k}^{(1)}, X_{1:k}^{(2)} | Z_{1:k}^{(1)}, Z_{1:k}^{(2)}, U_{1:k}^{(1)}, U_{1:k}^{(2)}, X_0^{(1)}, X_0^{(2)}) \end{aligned} \quad (2)$$

This factorization makes it possible to propagate the joint vehicle trajectories posterior using a particle filter that can accommodate complex non-linear motion models. Moreover, by representing the measurements and the landmark map as RFSs and modelling the landmark map transition model using finite set statistical (FISST) methods, it is possible to evaluate the landmark map posterior in the presence of false measurements (clutter) with data association and landmark detection uncertainty.

A. RFS Landmark Map Transition Model

Let the RFS representing the landmark map at time $k-1$ be denoted by M_{k-1}, then the landmark map transition model at time k is given by,

$$M_k = \Gamma_k(X_k^{(1)}, X_k^{(2)}) \cup \left[\bigcup_{\zeta_{k-1} \in M_{k-1}} \Upsilon(\zeta_{k-1}) \right] \quad (3)$$

where the RFS $\Gamma_k(X_k^{(1)}, X_k^{(2)})$ denotes the newly appearing landmarks in the joint sensor FOV, while the Bernoulli RFS $\Upsilon(\zeta_{k-1})$ denotes the predicted state of the landmark $\zeta_{k-1} \in M_k$.

B. RFS Landmark Measurement Model

Let M_k denote the predicted landmark map, while $C_k^{(r)}$ denote the RFS representing the clutter received from exteroceptive sensor mounted on rth vehicle at time k, then corresponding measurements can be represented by the RFS,

$$Z_k^{(r)} = C_k^{(r)} \cup \left[\bigcup_{\zeta_k \in M_k} \Theta_k^{(r)}(\zeta_k) \right] \quad (4)$$

where $\Theta_k^{(r)}(\zeta_k)$ is a Bernoulli RFS representing the measurement corresponding to landmark $\zeta_k \in M_k$.

IV. The PHD filter for Landmark Map Posterior Estimation

The landmark map posterior conditioned on the vehicle trajectories is evaluated using a PHD filter [12]. Let the PHD of the landmark map posterior at time k is given by,

$$\begin{aligned} &D_{k|k}(\zeta_k | Z_{1:k}^{(1)}, Z_{1:k}^{(2)}, X_{0:k}^{(1)}, X_{0:k}^{(2)}) \\ &= \int p_{k|k}(M_k \cup \zeta_k | Z_{1:k}^{(1)}, Z_{1:k}^{(2)}, X_{0:k}^{(1)}, X_{0:k}^{(2)}) \delta M_k \end{aligned} \quad (5)$$

then the number of landmarks in the map M_k in a region S can be obtained by,

$$N_{k|k} = \int_S D_{k|k}(\zeta_k | Z_{1:k}^{(1)}, Z_{1:k}^{(2)}, X_{0:k}^{(1)}, X_{0:k}^{(2)}) d\zeta_k \quad (6)$$

A. Landmark Map Prediction

The landmark map prediction posterior density is given by,

$$\begin{aligned} &p_{k|k-1}(M_k | Z_{1:k-1}^{(1)}, Z_{1:k-1}^{(2)}, X_{0:k}^{(1)}, X_{0:k}^{(2)}) \\ &= \int f_M(M_k | M_{k-1}, X_k^{(1)}, X_k^{(2)}) \\ &\times p_{k-1}(M_{k-1} | Z_{1:k-1}^{(1)}, Z_{1:k-1}^{(2)}, X_{0:k-1}^{(1)}, X_{0:k-1}^{(2)}) \delta M_{k-1} \end{aligned} \quad (7)$$

and the corresponding predicted PHD can be obtained using the PHD of the landmark map at time $k-1$ as,

$$\begin{aligned} &D_{k|k-1}(\zeta_k | Z_{1:k-1}^{(1)}, Z_{1:k-1}^{(2)}, X_{0:k}^{(1)}, X_{0:k}^{(2)}) \\ &= b_k(\zeta_k | X_k^{(1)}, X_k^{(2)}) \\ &+ D_{k-1|k-1}(\zeta_k | Z_{1:k-1}^{(1)}, Z_{1:k-1}^{(2)}, X_{0:k-1}^{(1)}, X_{0:k-1}^{(2)}) d\zeta_{k-1} \end{aligned} \quad (8)$$

where $b_k(\zeta_k | X_k^{(1)}, X_k^{(2)})$ denotes the intensity of the newly appearing landmarks in the joint sensor FOV.

B. Landmark Map Update

The landmark map update posterior density is given by,

$$\begin{aligned} &p_{k|k}(M_k | Z_{1:k}^{(1)}, Z_{1:k}^{(2)}, X_{0:k}^{(1)}, X_{0:k}^{(2)}) \\ &= g_k(Z_k^{(1)}, Z_k^{(2)} | M_k, X_k^{(1)}, X_k^{(2)}) \\ &\times \frac{p_{k|k-1}(M_k | Z_{1:k-1}^{(1)}, Z_{1:k-1}^{(2)}, X_{0:k}^{(1)}, X_{0:k}^{(2)})}{l_{k|k-1}(Z_k^{(1)}, Z_k^{(2)} | Z_{1:k-1}^{(1)}, Z_{1:k-1}^{(2)}, X_{0:k}^{(1)}, X_{0:k}^{(2)})} \end{aligned} \quad (9)$$

Assuming the number of false measurements produced by each vehicle is Poisson distributed at an average of $\lambda^{(r)}$, and their physical distribution given by $c^{(r)}(z^{(r)})$, the corresponding updated PHD can be obtained using two methods as follows.

1) Iterative update method: The resultant PHD can be obtained by iteratively updating the predicted PHD (8) [13] using each vehicles' observations as follows.

$$\begin{aligned} &D_{k|k}^{(1)}(\zeta_k | Z_{1:k}^{(1)}, Z_{1:k-1}^{(2)}, X_{0:k}^{(1)}, X_{0:k}^{(2)}) \\ &= (1 - P_D^{(1)}) D_{k|k-1}(\zeta_k) \\ &+ \sum_{z^{(1)} \in Z_k^{(1)}} \frac{P_D^{(1)} g_k^{(1)}(z^{(1)}) D_{k|k-1}(\zeta_k)}{\lambda^{(1)} c^{(1)}(z^{(1)}) + \int P_D^{(1)} g_k^{(1)}(z^{(1)}) D_{k|k-1}(\zeta_k) d\zeta_k} \end{aligned} \quad (10)$$

and

$$D^{(2)}_{k|k}(\zeta_k|Z^{(1)}_{1:k}, Z^{(2)}_{1:k} X^{(1)}_{0:k}, X^{(2)}_{0:k}) = (1 - P^{(2)}_D) D^{(1)}_{k|k}(\zeta_k) + \sum_{z^{(2)} \in Z^{(2)}_k} \frac{P^{(2)}_D g^{(2)}_k(z^{(2)}) D^{(1)}_{k|k}(\zeta_k)}{\lambda^{(2)} c^{(2)}(z^{(2)}) + \int P^{(2)}_D g^{(2)}_k(z^{(2)}) D^{(1)}_{k|k}(\zeta_k) d\zeta_k} \tag{11}$$

where, the abbreviations $D_{k|k-1}(\zeta_k)$ and $D^{(1)}_{k|k}(\zeta_k)$ are given by,

$$D_{k|k-1}(\zeta_k) = D_{k|k-1}(\zeta_k|Z^{(1)}_{1:k-1}, Z^{(2)}_{1:k-1}, X^{(1)}_{0:k}, X^{(2)}_{0:k}) \tag{12}$$

$$D^{(1)}_{k|k}(\zeta_k) = D^{(1)}_{k|k}(\zeta_k|Z^{(1)}_{1:k}, Z^{(2)}_{1:k-1} X^{(1)}_{0:k}, X^{(2)}_{0:k}) \tag{13}$$

and, $P^{(1)}_D$, $P^{(2)}_D$, $g^{(1)}_k(z^{(1)})$ and $g^{(2)}_k(z^{(1)})$ are given by,

$$P^{(1)}_D = P^{(1)}_D(\zeta_k|X^{(1)}_k), \quad P^{(2)}_D = P^{(2)}_D(\zeta_k|X^{(2)}_k) \tag{14}$$

$$g^{(1)}_k(z^{(1)}) = g^{(1)}_k(z^{(1)}|\zeta_k, X^{(1)}_k) \tag{15}$$

$$g^{(2)}_k(z^{(2)}) = g^{(2)}_k(z^{(2)}|\zeta_k, X^{(2)}_k) \tag{16}$$

where $P^{(r)}_D$ denotes the probability of detection of a landmark by rth vehicle which is often considered as a constant, while $g^{(r)}_k(z^{(r)})$ is the measurement likelihood function.

Hence the PHD of the measurement updated landmark map posterior (5) is approximated as,

$$D_{k|k}(\zeta_k|Z^{(1)}_{1:k}, Z^{(2)}_{1:k}, X^{(1)}_{0:k}, X^{(2)}_{0:k}) \approx D^{(2)}_{k|k}(\zeta_k|Z^{(1)}_{1:k}, Z^{(2)}_{1:k}, X^{(1)}_{0:k}, X^{(2)}_{0:k}) \tag{17}$$

This is a less computationally intensive approach for evaluating the PHD of the landmark map update posterior. Although computationally efficient, this method produces different PHDs under reordering of the sensor updates.

2) General multi-sensor update method: The PHD update can be obtained using the general multi-sensor update method [17] as follows,

$$D_{k|k}(\zeta_k|Z^{(1)}_{1:k}, Z^{(2)}_{1:k}, X^{(1)}_{0:k}, X^{(2)}_{0:k}) = (1 - P^{(1)}_D)(1 - P^{(2)}_D) D_{k|k-1}(\zeta_k) + \left[\sum_{\mathcal{P} \boxminus_2 Z_k} \omega_{\mathcal{P}} \sum_{W \in \mathcal{P}} \rho_W(\zeta_k) \right] D_{k|k-1}(\zeta_k) \tag{18}$$

where the summation is taken over all so called "binary partitions" $\mathcal{P}$ of $Z_k = Z^{(1)}_k \cup Z^{(2)}_k$ (see [17] for more information). The notation, "$\mathcal{P} \boxminus_2 Z_k$" stands for "$\mathcal{P}$ partitions Z_k into binary cells W", where $W \in \mathcal{P}$ has one of the following forms,

$$W = \left\{ z^{(1)}_k \right\}, \; W = \left\{ z^{(2)}_k \right\}, \; W = \left\{ z^{(1)}_k, z^{(2)}_k \right\} \tag{19}$$

The values of $\rho_W(\zeta_k)$ and $\omega_{\mathcal{P}}$ are given by,

$$\rho_W(\zeta_k) = \begin{cases} \dfrac{P^{(1)}_D l^{(1)}_{z^{(1)}}(\zeta_k)(1 - P^{(2)}_D)}{1 + D_{k|k-1}[P^{(1)}_D l^{(1)}_{z^{(1)}}(1 - P^{(2)}_D)]} & if \; W = \{z^{(1)}_k\} \\ \dfrac{(1 - P^{(1)}_D) l^{(2)}_{z^{(2)}}(\zeta_k) P^{(2)}_D}{1 + D_{k|k-1}[(1 - P^{(1)}_D) l^{(2)}_{z^{(2)}} P^{(2)}_D]} & if \; W = \{z^{(2)}_k\} \\ \dfrac{P^{(1)}_D l^{(1)}_{z^{(1)}}(\zeta_k) P^{(2)}_D l^{(2)}_{z^{(2)}}(\zeta_k)}{1 + D_{k|k-1}[P^{(1)}_D l^{(1)}_{z^{(1)}} P^{(2)}_D l^{(2)}_{z^{(2)}}]} & if \; W = \{z^{(1)}_k, z^{(2)}_k\} \end{cases} \tag{20}$$

and,

$$\omega_{\mathcal{P}} = \frac{\prod_{W \in \mathcal{P}} d_W}{\sum_{\mathcal{Q} \boxminus_2 Z_k} \prod_{W \in \mathcal{Q}} d_W} \tag{21}$$

where,

$$l^{(1)}_{z^{(1)}}(\zeta_k) = \frac{g^{(1)}_k(z^{(1)}_k|\zeta_k, X^{(1)}_k)}{\lambda^{(1)}_k c^{(1)}_k(z^{(1)}_k)} \tag{22}$$

$$l^{(2)}_{z^{(2)}_k}(\zeta_k) = \frac{g^{(2)}_k(z^{(2)}_k|\zeta_k, X^{(2)}_k)}{\lambda^{(2)}_k c^{(2)}_k(z^{(2)}_k)} \tag{23}$$

and,

$$d_W = \begin{cases} 1 + D_{k|k-1}[P^{(1)}_D l^{(1)}_{z^{(1)}}(1 - P^{(2)}_D)] & if \; W = \{z^{(1)}_k\} \\ 1 + D_{k|k-1}[(1 - P^{(1)}_D) l^{(1)}_{z^{(1)}} P^{(2)}_D] & if \; W = \{z^{(2)}_k\} \\ 1 + D_{k|k-1}[P^{(1)}_D l^{(1)}_{z^{(1)}} P^{(2)}_D l^{(2)}_{z^{(2)}}] & if \; W = \{z^{(1)}_k, z^{(2)}_k\} \end{cases} \tag{24}$$

For any function $h(\zeta_k)$, $D_{k|k-1}[h(\zeta_k)]$ is given by,

$$D_{k|k-1}[h(\zeta_k)] = \int h(\zeta_k) D_{k|k-1}(\zeta_k) d\zeta_k \tag{25}$$

As usual $P^{(r)}_D = P^{(r)}_D(\zeta_k|X^{(r)}_k)$ denotes the probability of detection of a landmark ζ_k, by rth vehicle and is considered as a constant whose value depends on W. If W is a singleton observation, then the probability of detection of the corresponding sensor is set higher than the other. If W contains two elements, that suggests the observation received is from a feature in the overlapping area of the sensor FOVs and hence the probability of detection of both sensor are set to a higher constant.

Although computationally more demanding, this approach produces an invariant PHD for any ordering of the sensor updates. Computational load can be minimized using sensor consistency gating [17].

C. Implementation of the PHD filter

The PHD prediction and udpate equations are implemented using a GM implementation of the PHD filter [16]. The PHD of the landmark map posterior at time $k-1$ and the newly appearing landmarks in the joint sensor FOV are represented by a mixture of Gaussians, then the resultant measurement updated PHD at time k can be obtained as a mixture of Gaussian components from which the landmark locations and the number of landmarks can be obtained [16] in order to solve the MVSLAM problem.

V. Particle Filter for Joint Vehicle Trajectories and Landmark Map Posterior Estimation

The joint vehicle trajectories posterior is evaluated using a particle filter, which can be represented by a set of weighted particles denoted by Ω_k as follows,

$$\Omega_k = \left\{ w_k^{[i]}, X_{1:k}^{(1),[i]}, X_{1:k}^{(2),[i]} \right\}_{i=1}^{N_s} \tag{26}$$

where, N_s denotes the number of particles and $w_k^{[i]}$ is the weight of ith particle which can be obtained as,

$$\begin{aligned} & w_k^{[i]} \\ & \propto l_{k|k-1}(Z_k^{(1)}, Z_k^{(2)} | Z_{1:k-1}^{(1)}, Z_{1:k-1}^{(2)}, X_{0:k}^{(1),[i]}, X_{0:k}^{(2),[i]}) \end{aligned} \tag{27}$$

where $l_{k|k-1}(Z_k^{(1)}, Z_k^{(2)} | Z_{1:k-1}^{(1)}, Z_{1:k-1}^{(2)}, X_{0:k}^{(1)}, X_{0:k}^{(2)})$ is the normalization constant in (9). Assuming the number of elements in M_k is Poisson distributed, extending the approach proposed by Mullane et al. in [14] [15], it can be shown that,

$$\begin{aligned} & l_{k|k-1}(Z_k^{(1)}, Z_k^{(2)} | Z_{1:k-1}^{(1)}, Z_{1:k-1}^{(2)}, X_{0:k}^{(1)}, X_{0:k}^{(2)}) \\ & = \prod_{z^{(1)} \in Z_k^{(1)}} \lambda^{(1)} c^{(1)}(z^{(1)}) \prod_{z^{(2)} \in Z_k^{(2)}} \lambda^{(2)} c^{(2)}(z^{(2)}) \\ & \times \exp(N_{k|k} - N_{k|k-1} - \lambda^{(1)} - \lambda^{(2)}) \end{aligned} \tag{28}$$

where $N_{k|k-1}$ and N_k respectively denote the number of landmarks present in the predicted landmark map and the number of landmarks present after updating the landmark map.

Now since the PHD of the landmark map posterior is conditioned on the joint vehicle trajectories, the joint landmark map and vehicle trajectories posterior at time k can be written as,

$$\left\{ w_k^{[i]}, X_k^{(1),[i]}, X_k^{(2),[i]}, D_{k|k}(\zeta_k | Z_{1:k}^{(1)}, Z_{1:k}^{(2)}, X_{0:k}^{(1),[i]}, X_{0:k}^{(2),[i]}) \right\}_{i=1}^{N_s} \tag{29}$$

VI. Simulation Results

Performance of the proposed MVSLAM algorithms are evaluated using simulations and the results are benchmarked against the MVSLAM algorithm proposed by Howard [4]. From here onwards the proposed MVSLAM solutions are referred to as RFS-MVSLAM-I and RFS-MVSLAM-II respectively denoting the solutions based on iterative update method and the general multi-sensor update method, while the benchmarked MVSLAM solution by Howard is referred to as RB-MVSLAM. In order to improve the performance under measurement clutter, the RB-MVSLAM algorithm is combined with a real-time implementation of feature elimination method based on negative evidence strategy proposed by Montemerlo [9].

Two vehicles with identical control and sensor parameters (given in Table.I) are driven on two different trajectories on a simulation environment consisting of 41 randomly place landmarks. It is assumed that the number of false measurements generated by each vehicle is Poisson distributed and posess a uniform spatial distribution in the sensor FOV. Probability of detection of a landmark is assumed to be constant and set to 0.99 and probability of survival of a landmark from current time step to the next is also assumed to be constant and set to 0.99.

TABLE I
Parameters Used in the Simulation

Vehicle Parameters		Values
Velocity	V	4m/s
Sensor FOV	Range (r)	0 - 120m
	Bearing (b)	$-\pi/2$ - $+\pi/2$
Control Noise	Velocity (σ_v)	0.3m/s
	Steering Angle (σ_α)	2^0
Measurement Noise	Range (σ_r)	0.3m
	Bearing (σ_b)	0.5^0

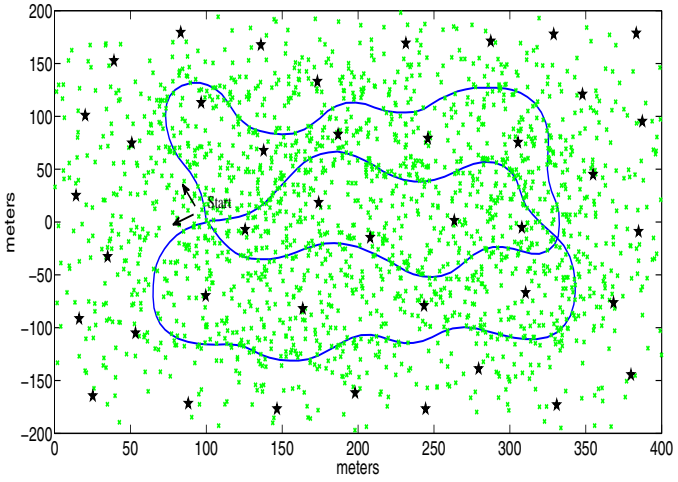

(a) Low clutter condition ($\lambda^{(r)} = 1$)

Fig. 1. Ground truth of the vehicle trajectories (in blue) with randomly placed landmarks (black stars) under low ($\lambda^{(r)} = 1$) clutter (in green) condition, where $r = 1, 2$ denotes the vehicle number. The number of landmarks present in the simulation enviornment is 41.

VII. Conclusion

In this paper we have presented a novel Multi-Vehicle SLAM (MVSLAM) solution by extending the RFS based SLAM filter framework using two recently developed multi-sensor fusion techniques in finite set statistics (FISST). The RFS representation of the landmark map and measurements enables modelling of the landmark map transition model and observation model in a more natural manner, resulting a Bayesian MVSLAM algorithm with inbuilt map management, data association and clutter filtering. The performance characteristics obtained via the simulation results suggests that the proposed solutions produces robust results under false measurements with data association and landmark detection uncertainty.

Acknowledgment

This work was supported by National Research Foundation (NRF), Singapore and Center for Environmental Sensing and Modeling (CENSAM) under the auspices of the Singapore-MIT Alliance for Research and Technology (SMART). The

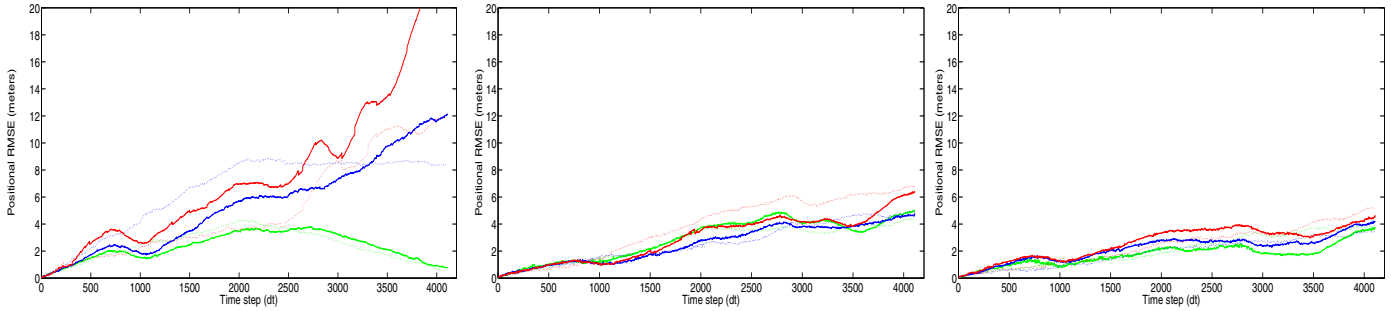

(a) RB-MVSLAM (b) RFS-MVSLAM-I (c) RFS-MVSLAM-II

Fig. 2. RMS Vehicle position errors of 10 MC runs under low (in green), mild (in blue) and high (in red) clutter conditions. Dotted graphs corresponds to the first vehicle, while the non-dotted graphs corresponds to the second vehicle.

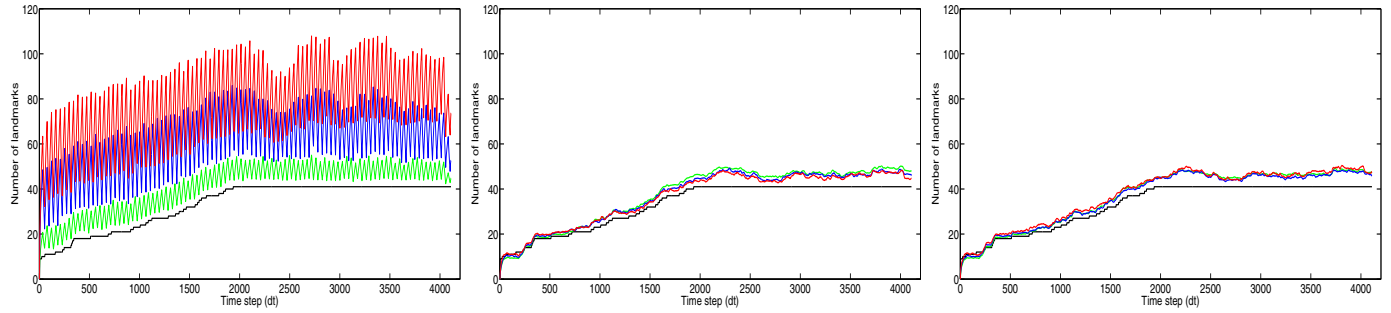

(a) RB-MVSLAM (b) RFS-MVSLAM-I (c) RFS-MVSLAM-II

Fig. 3. Average number of landmarks in the map under low (in green), mild (in blue) and high (in red) clutter conditions, superimposed on the actual number of landmarks (in black).

work of B.-N. Vo is supported by Australian Research Council under the Future Fellowship FT0991854.

REFERENCES

[1] J.W. Fenwick, P.M. Newman and J.J. Leonard, "Cooperative Concurrent Mapping and Localization," in *Proc. IEEE Int. Conf. Robot. Autom.*, August 2002, pp. 1810–1817.

[2] S.B. Williams, G. Dissanayake and H. Durrant-Whyte, "Towards multi-vehicle simultaneous localization and mapping," in *Proc. IEEE Int. Conf. Robot. Autom.*, August 2002, pp. 2743–2748.

[3] S. Thrun and Y. Liu, "Multi-robot SLAM with sparse extended information filters," in *Proc. Int. Symp. Robot. Res.*, Sienna, Italy, October 2003, pp. 254–266.

[4] A. Howard, "Multi-robot simultaneous localization and mapping using Particle Filters," *The Int. J. Robot. Res.*, vol. 25, no. 12, pp. 1243–1256, December 2006.

[5] D. Fox, J. Ko, K. Konolige, B. Limketkai, D. Schulz and B. Stewart, "Distributed Multirobot Exploration and Mapping," *Proc. IEEE*, vol. 94, no. 7, pp. 1325–1339, July 2006.

[6] X. Zhou and S. Roumeliotis, "Multi-robot SLAM with unknown initial correspondence: the robot rendezvous case," in *Proc. IEEE/RSJ Int. Conf. Intell. Robot. Sys.*, Oct 2006, pp. 1785–1792.

[7] L. Carlone, M.K. Ng, J. Du, B. Bona and M. Indri, "Rao-Blackwellized Particle Filters Multi Robot SLAM with Unknown Initial Correspondences and Limited Communication," in *Proc. IEEE Int. Conf. Robot. Autom.*, May 2010, pp. 243–249.

[8] G. Dissanayake, P.M. Newman, S. Clark, H. Durrant-Whyte and M. Csorba, "A Solution to the Simultaneous Localization and Map Building (SLAM) Problem," *IEEE Trans. Robot. Autom.*, vol. 17, no. 3, pp. 229–241, June 2001.

[9] M. Montemerlo, "FastSLAM: a factored solution to the simultaneous localization and mapping problem with unknown data association," Ph.D. dissertation, School of Computer Science, Carnegie Melon University, 2003.

[10] S. Thrun, Y. Liu, D. Koller, A.Y. Ng, Z. Ghahramani and H. Durrant-Whyte, "Simultaneous Localization and Mapping with Sparse Extended Information Filters," *The Int. J. Robot. Res.*, vol. 23, no. 7-8, pp. 693–716, August 2004.

[11] J. Mullane, B.N. Vo, M.D. Adams and W.S. Wijesoma, "A Random Set Formulation for Bayesian SLAM," in *Proc. IEEE/RSJ Int. Conf. Intell. Robot. Syst.*, September 2008, pp. 1043–1049.

[12] R. Mahler, "Multitarget Bayes Filtering via First-Order Multitarget Moments," *IEEE Trans. Aerosp. Electron. Syst.*, vol. 39, no. 4, pp. 1152–1178, January 2004.

[13] ——, *Statistical Multisource-Multitarget Information Fusion*. Norwood, MA: Artech House, 2007.

[14] J. Mullane, B.N. Vo and M.D. Adams, "Rao-Blackwellised PHD SLAM," in *Proc. IEEE Int. Conf. Robot. Autom.*, May 2010, pp. 5410–5416.

[15] J. Mullane, B.N. Vo, M.D. Adams and B.T. Vo, "A Random-Finite-Set Approach to Bayesian SLAM," *IEEE Trans. Robot. Autom.*, vol. 27, no. 2, pp. 268–282, February 2011.

[16] B.N. Vo and W.K. Ma, "The Gaussian Mixture Probability Hypothesis Density Filter," *IEEE Trans. Signal Process.*, vol. 54, no. 11, pp. 4091–4104, November 2006.

[17] R. Mahler, "The multisensor PHD filter: I. General solution via multi-target calculus," in *Proc. SPIE Sig. Process., Sensor Fusion., and Target Recog. XVIII*. SPIE, April 2009, pp. 1043–1049.

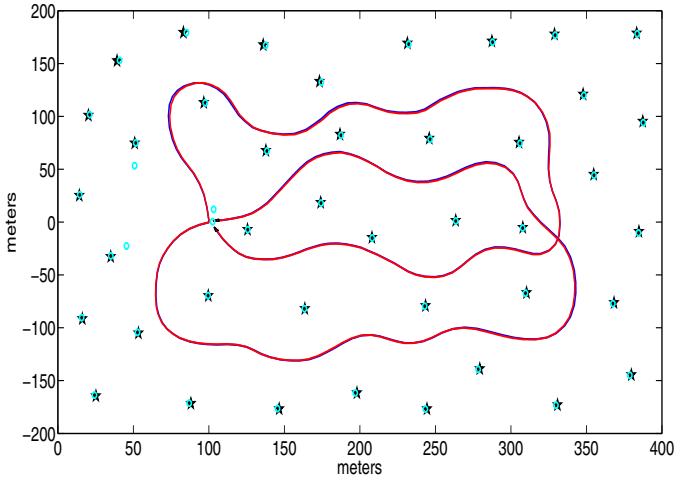

(a) RB-MVSLAM with $\lambda^{(r)} = 1$

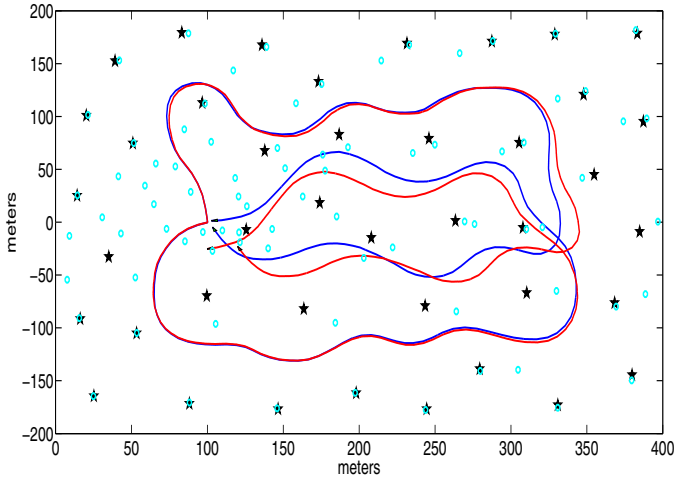

(b) RB-MVSLAM with $\lambda^{(r)} = 10$

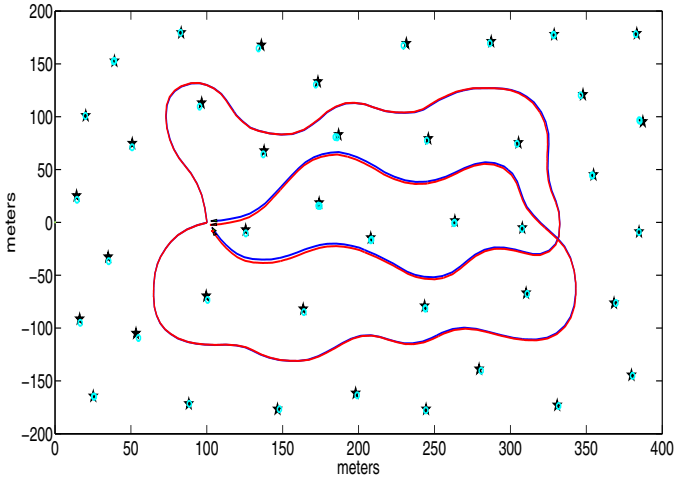

(c) FISST-MVSLAM-I with $\lambda^{(r)} = 1$

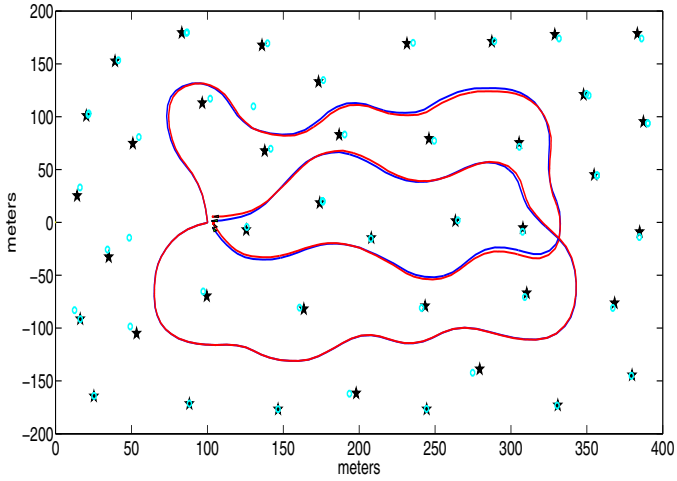

(d) RFS-MVSLAM-I with $\lambda^{(r)} = 10$

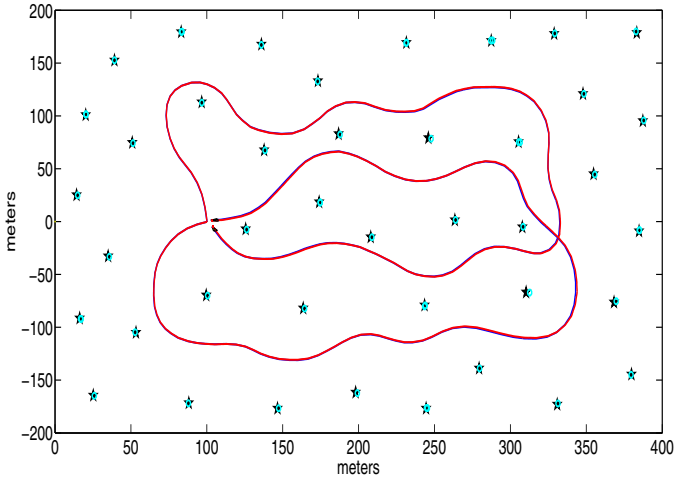

(e) RFS-MVSLAM-II with $\lambda^{(r)} = 1$

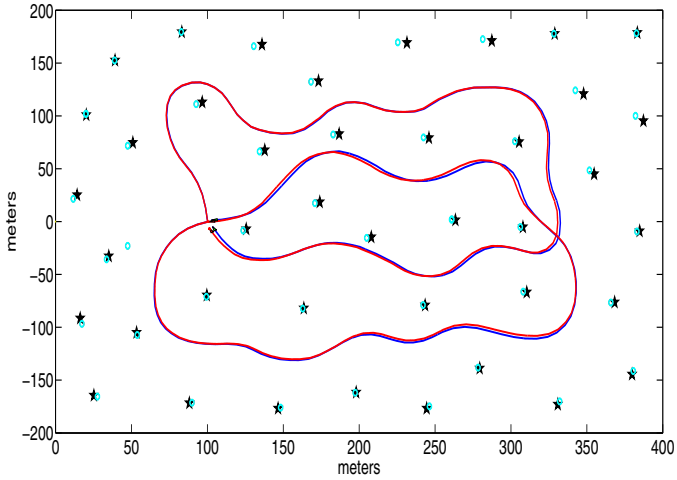

(f) RFS-MVSLAM-II with $\lambda^{(r)} = 10$

Fig. 4. A comparison of estimated vehicle trajectories (in red), superimposed on ground truth (in blue) with estimated features (cyan circles) and actual features (black stars), of a sample run of each algorithm under low and high clutter conditions.